Effects of CO_2 Sorption on the Rotational Reorientation Dynamics of a Model Solute Dissolved in Molten Poly(dimethylsiloxane)

Emily D. Niemeyer and Frank V. Bright*

Department of Chemistry, Natural Sciences Complex, State University of New York at Buffalo, Buffalo, New York 14260-3000

Received March 11, 1997; Revised Manuscript Received November 6, 1997[⊗]

ABSTRACT: We report on the effects of polymer molecular weight, temperature, and near- and supercritical CO_2 gas sorption on the rotational reorientation dynamics of a model solute (BTBP) dissolved in molten poly(dimethylsiloxane) (PDMS). In order to determine the BTBP rotational dynamics, we have carried out time-resolved fluorescence anisotropy measurements in PDMS polymers of varying molecular weight. These results show that there is a linear correlation between the BTBP rotational reorientation dynamics and the PDMS polymer bulk density. Temperature-dependent studies of the BTBP/PDMS system shows that the BTBP rotational reorientation dynamics are accurately described by an Arrhenius activation model. The recovered activation energies for the BTBP dynamics are statistically the same as the activation energy for PDMS viscous flow. The addition of CO_2 to the BTBP/PDMS system leads to an appreciable decrease in the BTBP rotational reorientation time with CO_2 pressure. These results illustrate how polymer dilation by CO_2 can be used to tailor the dynamics within polymer systems.

Introduction

There is significant interest in tailoring polymer formation, modification, and processing.[1] Of particular recent interest has been the use of near-critical/supercritical fluids to tune polymer molecular weight and molecular weight distributions during polymerization reactions,[2] modify bulk polymer viscosity,[3] achieve selective extraction, fractionation, and/or separations,[4] dope or impregnate polymers,[5] selectively precipitate polymers by expansion from a supercritical fluid,[6] and carry out polymerizations within polymer systems.[7] Much of this work is motivated because certain fluids (e.g., CO_2) are environmentally attractive alternatives to common liquids[8] and the physicochemical properties of a supercritical fluid can be adjusted continuously with pressure.[9]

It is well-known that pressurized gases can be used to alter the physicochemical properties of certain polymers.[10] Carbon dioxide in particular swells many polymers and depresses their glass transition temperature (T_g).[1,10] Recent work has also shown that molten polymers like poly(dimethylsiloxane) (PDMS) can sorb tremendous amounts of CO_2 (up to 40% by weight), leading to a dramatic decrease in the bulk polymer viscosity and significantly increased dilation.[3] PDMS is a unique, silicone-based polymer that possesses a glass transition temperature (T_g) around 150 K, exhibits good hydrolytic, oxidative, pH, and thermal stability, and has been used extensively for coatings, in implants, and as hydraulic fluids.[11]

Researchers have developed and used several instrumental methods to investigate the behavior of "probes" within polymer systems.[12−19] In most of this work the primary goal has been to determine how the polymer affects the probe/dopant cybotactic region (i.e., the local environment surrounding the probe molecule that is sensed by the probe molecule) and/or recover the time-dependent probe orientational correlation function.[12−19] Most recent work has used dielectric,[12] nuclear magnetic resonance,[13] electron spin resonance,[14] electronic absorbance,[15] second harmonic generation,[16] photobleaching,[17] static fluorescence,[18] and/or time-resolved fluorescence methods.[19] Time-resolved fluorescence anisotropy measurements are particularly attractive because they allow one to work under conditions where the probe loading within the polymer is low and they provide an intrinsic reference length scale (the fluorophore's dimension). To date, time-resolved fluorescence anisotropy methods have been used to investigate fluorophore−polymer interactions in the bulk,[19b] to follow subunit dynamics,[18a,19a,d,i,k,20] and to track the motion of the elastic cross-link junction[18h,19g,l,o] within various polymers.

Of particular interest to the current work is temperature-dependent work by Chu and Thomas on pyrene intermolecular excimer formation in PDMS,[19e] the Pajot-Augy et al. work on 10,10′-diphenylenebis(9-anthrylmethyl oxide) intramolecular excimer formation in PDMS,[18c] work by Fayer and his associates on *N*-((triethoxysilyl)propyl)dansylamide (DTES)[19g] and *N*-((triethoxysilyl)propyl)naphthalene (NTES)[19i,p] attached directly to PDMS network junction sites, and work by Stein et al. on DTES dispersed in PDMS.[19h] Pajot-Augy et al.[18c] and Chu and Thomas[19e] reported that the activation energy for intermolecular excimer formation in PDMS is 15.9 and 16.2 kJ/mol, respectively. Fayer's group[19g] found that the activation energy associated with the rotational reorientation of DTES dispersed randomly in PDMS was 27 kJ/mol. In contrast, the activation energies associated with the rotational reorientation of DTES or NTES attached covalently to a PDMS network junction point were found to be 19 ± 2 kJ/mol[19g] or 11.4 ± 0.8 kJ/mol,[19i,p] respectively. As a benchmark, the activation energy for PDMS viscous flow is reportedly 16 ± 1 kJ/mol.[19h,21]

* Author to whom all correspondence should be addressed. Voice: 716-645-6800, ext. 2162. Fax: 716-645-6963. E-mail: chefvb@acsu.buffalo.edu.

[⊗] Abstract published in *Advance ACS Abstracts,* December 15, 1997.

S0024-9297(97)00335-5 CCC: $15.00
Published on Web 01/13/1998

Interestingly, in many other polymer systems, over a broad temperature range, it has been shown that the activation energy to viscous flow and the activation to probe rotational reorientation are, within experimental uncertainties, equal.[16,17,19f] Thus, the local probe dynamics generally correlate well with the dynamics leading to polymer viscous flow. However, for certain probes in PDMS (DTES and NTES dispersed or bound covalently) it appears there is some deviation between the activation energetics for probe reorientation and viscosity.

In this paper we use the frequency-domain fluorescence technique[22] to determine the time-resolved anisotropy decay kinetics of a large organic probe dispersed randomly in PDMS polymers. The probe used for the current work is *N*,*N*′-bis(2,5-di-*tert*-butylphenyl)-3,4,9,10-perylenedicarboximide (BTBP). BTBP was chosen for several reasons.[23] First, BTBP has a molar volume (733 Å^3) which is almost twice that of any other fluorescent probe used to study PDMS. Second, BTBP has been used previously to investigate solute−fluid frictional forces and dynamics within a variety of media. Third, BTBP is not charged nor is it polar, so there should be few if any specific interactions with the polymer matrix. Fourth, BTBP has a unity fluorescence quantum yield and its intensity decay kinetics are described well by a single exponential rate law. Finally, BTBP is an isotropic rotor and its rotational reorientation dynamics are well-described by a single rotational reorientation time in many different environments.[23] This final feature should be contrasted with much of the aforementioned work with PDMS where the probe fluorescence anisotropy decay kinetics were intrinsically anisotropic[19h,i,g,p] and thus more difficult to interpret.[24]

The experiments described in this paper are divided into four parts. As a jumping point we characterize the BTBP rotational reorientation dynamics in eight PDMS polymers of varying average molecular weight (M_W). The goals of these experiments are to determine the following: (1) the form of the orientational correlation function and (2) how the BTBP rotational motion correlates with bulk polymer properties. We next measure the BTBP rotational reorientation time as a function of M_w and temperature to determine if the probe reorientation is correlated with the activation energy for PDMS viscous flow (E_η). In a third series of experiments, we determine how the volume fraction of a solvent (toulene), added to the PDMS polymer, affects the BTBP rotational reorientation dynamics. Lastly, we determine how CO_2 pressure (between 0 and 2500 psia) and temperature (25 and 37 °C) affect the rotational reorientation dynamics of BTBP dissolved in PDMS polymers.

Experimental Section

Materials and Reagents. A broad average molecular weight range of methyl-terminated PDMS was purchased from United Chemical Technologies, Inc. (Bristol, PA) and used without further purification. The physicochemical properties of these particular polymers are listed in Table 1. *N*,*N*′-bis-(2,5-di-*tert*-butylphenyl)-3,4,9,10-perylenedicarboximide (BTBP, structure shown in the top panel inset of Figure 1) (Aldrich) and anhydrous toluene (HPLC grade, Sigma) were also used as received. Supercritical fluid chromatographic grade CO_2 was purchased from Scott Specialty Gases and was further purified by passage through an in-line oxygen trap (Matheson).

Preparation of Polymer Samples. Stock solutions of BTBP (1 mM) were prepared in absolute ethanol. BTBP is dissolved within the PDMS polymer samples by using the following procedure: (1) the appropriate amount of BTBP stock solution is micropipetted into a vial; (2) the vial is placed within a 100 °C oven for approximately 1 h to drive off all the ethanol; (3) after cooling, the appropriate quantity of PDMS is added directly to the vial such that the final BTBP/PDMS solution is 1 μM BTBP; (4) the solutions are stirred (with gentle heating for higher molecular weight samples) for approximately 2 weeks to ensure that the BTBP is fully dissolved in the PDMS. There is no evidence of BTBP aggregates nor decomposition.

Table 1. Physicochemical Properties of the Methyl-Terminated PDMS Polymers Used in This Work[a]

M_w[b] (g/mol)	η[c] (cP)	DP[d]	density (g/mL)	α[e] $\times 10^{-4}$ (K^{-1})
1250	10	14.7	0.935	10.8
2000	20	24.8	0.950	10.7
3780	50	48.8	0.960	10.6
5970	100	78.4	0.966	9.3
9430	200	125	0.968	9.3
13 650	350	182	0.970	9.3
28 000	1000	376	0.971	9.3
49 350	5000	664	0.973	9.3

[a] Data from *Silicon Compounds. Register and Review*, United Chemical Technologies, pp 254−255. [b] Polymer molecular weight. [c] Bulk viscosity at 20 °C. [d] Degree of polymerization (DP = [M_w − 162.18]/74.09). [e] Coefficient of thermal expansion.

For all temperature-dependent work, the sample temperature was controlled by a Lauda RLS-6 circulating bath. The actual polymer temperatures were determined using a solid-state thermocouple (Cole Parmer, Vernon Hills, IL) immersed directly within the quartz sample cuvette just prior to the spectroscopic measurement. The temperature was controlled to within ±0.1 °C.

To prepare the toluene/PDMS samples, an appropriate aliquot of neat toluene is added to the BTBP/PDMS solution (polymer M_w = 9430). The solution is mixed for 2 days to ensure that the samples are at equilibrium.

Addition of CO_2 to the Polymer Samples. Carbon dioxide is added to the polymer samples by using a microprocessor-controlled syringe pump to continuously deliver CO_2 to a high-pressure optical cell containing the BTBP/PDMS sample. The stainless steel high-pressure optical cell (5 mL internal volume) system was developed in-house and has been described in detail previously.[25] The cell optical windows are fused silica (Behm Quartz Industries), and they do not exhibit any detectable strain-induced birefringence over the pressure range studied in this work.[23c]

To prepare a sample for study, we add 3.75 mL of a BTBP/PDMS sample directly into the high-pressure optical cell. A teflon-coated stir bar is placed in the bottom of the optical cell to ensure efficient mixing. A valve assembly connects the optical cell to the high-pressure syringe pump (Isco, model 260D, Lincoln, NE). The pump is operated in the constant pressure mode. Throughout the experiment, a Haake A80 temperature bath is used to maintain the optical cell temperature (±0.1 °C) and the cell temperature is monitored using a solid-state thermocouple located in the cell body. Pressure is monitored within ±1 psi using a calibrated Heise gauge.

In a typical CO_2 experiment, we first charge the high-pressure optical cell (loaded already with BTBP/PDMS) to the highest pressure (~2500 psia) and allow the system to equilibrate at constant experimental temperature with constant stirring. Initially, BTBP/PDMS samples were equilibrated overnight before measurements were carried out. However, during the course of these preliminary experiments we encountered an inordinately large degree of imprecision between "replicate" measurements. On carefully evaluating these early data and their circumstances, we discovered that the system was *not* at equilibrium even *after* stirring 12 h. Figure 1 (upper panel) illustrates the time course of the BTBP rotational reorientation time in PDMS (M_w = 28 000) on the addition of 1078 psia of CO_2 at 25 °C. Time "0" corresponds to the system 12 h after initial CO_2 addition. These results show that there is an initial increase in the BTBP rotational

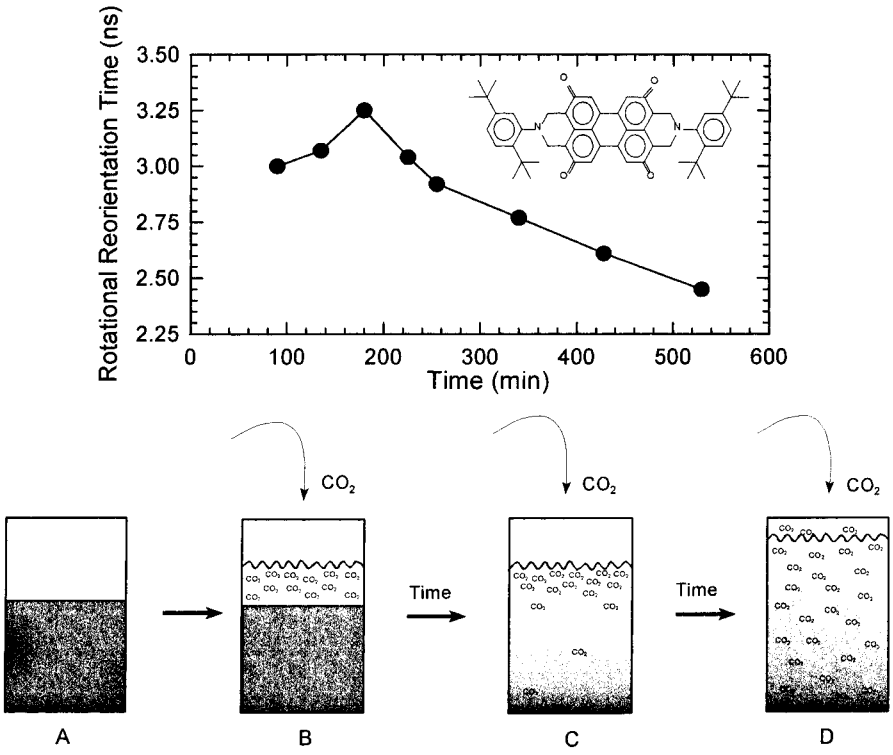

Figure 1. Time course of the BTBP dynamics in PDMS on being subjected to 1078 psia of CO_2 ($T = 25.0$ °C). (Panel A) Rotational reorientation time as a function of incubation time in 28 000 g/mol of PDMS. (A−D) Cartoons depicting PDMS/CO_2 interactions over time: (A) Neat polymer. (B) After initial CO_2 addition. (C) After time, the CO_2 begins to effuse into the PDMS and dilate the polymer. (D) At equilibrium the CO_2 has fully partitioned into the PDMS. The inset shows the chemical structure of BTBP.

reorientation time which we attribute to a primary compression of the PDMS on initial delivery of CO_2 to the high-pressure optical cell (panel A to panel B). As the PDMS polymer begins to take up the CO_2 (panels B and C), it begins to swell and dilate and we see a systematic decrease in the BTBP rotational reorientation time with equilibration time (panel C). At longer equilibration times, the polymer continues to absorb CO_2 until the system reaches equilibrium (panel D). The systematic decrease in the BTBP rotational reorientation time (upper panel) continued for up to 1 week. To ensure that all our PDMS/CO_2 samples were at equilibrium, all samples were mixed at constant temperature for at least 2 weeks before dynamical experiments were performed. There were no discrepancies or observable hysterisis when this protocol was adopted.

Instrumentation. All time-resolved fluorescence measurements[22] were made using a multiharmonic frequency-domain fluorometer (SLM-AMINCO 48000 MHF). The 514.5-nm line of a CW Ar^+ laser (Coherent, model Innova 400) was used as the excitation source. The output from the laser is directed through an interference filter to eliminate any extraneous plasma discharge from reaching the emission detector.

The sample fluorescence is monitored through a 550 long-pass filter and an excitation/emission polarizer pair is set at the magic angle[26] for all fluorescence lifetime measurements. Sinusoidally modulated light is generated using a Pockels cell driven at 5 MHz, and data are collected from 5 to 200 MHz (39 frequencies). At least nine replicate measurements were made on each sample. Rhodamine 6G in water was used as the reference lifetime standard for all excited-state fluorescence lifetime measurements ($\tau_{ref} = 3.85$ ns).[27] The BTBP fluorescence lifetime was, within our measurement uncertainty, constant over the range of experimental conditions used in this work.

Data Acquisition and Recovery of the Excited-State Intensity and Anisotropy Decays. *Excited-State Fluorescence Intensity Decays.* The general time course of the decay of fluorescence intensity ($I(t)$) following pulsed excitation is given by

$$I(t) = \sum_{i=1}^{n} \alpha_i e^{-t/\tau_i} \tag{1}$$

where α_i is the pre-exponential factor denoting the contribution to the total time-resolved decay of the ith component with lifetime τ_i. In the frequency domain,[22] the sample under study is excited with sinusoidally modulated light and the experimentally measured parameters are the frequency-dependent phase angle ($\Theta(\omega)$) and demodulation factor ($M(\omega)$). These values are compared by nonlinear regression to the values predicted from an assumed decay law, and the model parameters adjusted to yield minimal deviations between the data and the prediction. For any intensity decay (eq 1), the frequency-domain data are related to the observables through the sine and cosine Fourier transforms:

$$S(\omega) = \frac{\int I(t) \sin \omega t \, dt}{\int I(t) \, dt} \tag{2}$$

$$C(\omega) = \frac{\int I(t) \cos \omega t \, dt}{\int I(t) \, dt} \tag{3}$$

where ω is the angular modulation frequency ($\omega = 2\pi f$, f = linear modulation frequency) and

$$\Theta(\omega) = \arctan[S(\omega)/C(\omega)] \tag{4}$$

$$M(\omega) = [S(\omega)^2 + C(\omega)^2]^{1/2} \tag{5}$$

The decay terms (α_i and τ_i) are recovered from the experimental data by the nonlinear least squares regression subject to minimization of the χ^2 function:

$$\chi^2 = \frac{1}{D}\sum\left(\frac{\Theta(\omega) - \Theta_c(\omega)}{\delta\Theta}\right)^2 + \frac{1}{D}\sum\left(\frac{M(\omega) - M_c(\omega)}{\delta M}\right)^2 \tag{6}$$

In this expression D is the number of degrees of freedom, and $\delta\Theta$ and δM are the uncertainties in the measured phase angle and demodulation, respectively. The subscript c denotes the frequency-dependent phase and modulation calculated on the basis of α_i and τ_i and eqs 1−5.

Fluorescence Anisotropy Decay Kinetics. In the time domain the sample is excited with a brief pulse of polarized light and the time dependence of the parallel ($I_{||}(t)$) and perpendicular ($I_{\perp}(t)$) components of the fluorescence yield the time-resolved decay of anisotropy, $r(t)$:

$$r(t) = \frac{[I_{||}(t) - I_{\perp}(t)]}{[I_{||}(t) + 2I_{\perp}(t)]} \tag{7}$$

For a simple isotropic rotor $r(t)$ is described by a single rotational correlation time, ϕ:[1,2,20,23]

$$r(t) = r_0 \exp(-t/\phi) \tag{8}$$

where r_0 is the limiting anisotropy measured in the absence of rotational reorientation. For more complicated systems, $r(t)$ takes the following form:

$$r(t) = r_0 \sum \beta_i \exp(-t/\phi_i) \tag{9}$$

where β_i and ϕ_i are the fractional contribution of the total decay of anisotropy and the rotational correlation time attributed to reorientational motion, i, respectively.

In the frequency domain, the anisotropy decay kinetics are determined from frequency-dependent measurements of differential polarized phase angle Δ ($= \theta_{\perp} - \theta_{||}$) and the polarized modulation ratio Λ ($= m_{||}/m_{\perp}$).[22] If the time-dependent intensity decay is given by eq 1, the decay of the parallel and perpendicular components of the polarized fluorescence are written as follows:

$$I_{||}(t) = {}^1/_3[I(t)(1 + 2r(t))] \tag{10}$$

and

$$I_{\perp}(t) = {}^1/_3[I(t)(1 - r(t))] \tag{11}$$

Regardless of the form of $r(t)$, Δ and Λ are given by

$$\Delta = \arctan\left[\frac{D_{||}N_{\perp} - D_{\perp}N_{||}}{N_{||}N_{\perp} + D_{\perp}D_{||}}\right] \tag{12}$$

$$\Lambda = \left[\frac{N_{||}^2 + D_{||}^2}{N_{\perp}^2 + D_{\perp}^2}\right]^{1/2} \tag{13}$$

where N_i and D_i represent the polarized components of the sine and cosine Fourier transforms, respectively. The parameters of interest, β_i and ϕ_i, are subsequently recovered by fitting the frequency-dependent Δ and Λ data using nonlinear regression methods (*vide supra*).

Our frequency-domain rotational reorientation data sets were fit to various test models by using a commercially available global analysis software package (Globals Unlimited).[28] In all cases, frequency weighting was performed using the individual imprecision in each datum.

Results and Discussion

Rotational Reorientation Dynamics within PDMS Polymers at Ambient Temperature. Figure 2 presents typical differential polarized phase angle (panel A) and polarized modulation ratio (panel B) fluorescence data sets for BTBP in three PDMS molecular weight polymers at room temperature (21 ± 1 °C).

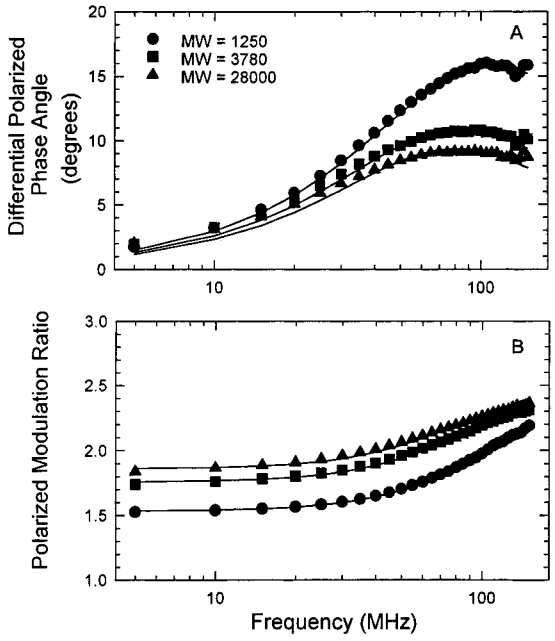

Figure 2. Typical frequency domain data for BTBP in PDMS. (Panel A) Differential polarized phase angle (Δ) as a function of frequency for BTBP in PDMS. (Panel B) Polarized modulation ratio (Λ) as a function of frequency for BTBP in PDMS.

A variety of models have been used to describe rotational reorientation of probes in bulk polymers.[19f] Among the most popular has been the stretched exponential:

$$r(t) = r_0[e^{-t/\phi}]^{\gamma} \tag{14}$$

In this expression, r_0 and ϕ have their usual meaning (*vide supra*) and γ is a measure of the heterogeneity of the reorientational process. Values of γ near unity suggest a narrow set of rotational reorientation processes whereas small γ values are consistent with a more broad distribution of probe reorientational processes.

The points in Figure 2 represent the experimental data and the solid curves denote the best fits to a single-exponential decay law (eq 8). Under *all* conditions investigated in this work, based on the fit quality, χ^2, and the residual between the model and the experimental data, the BTBP rotational reorientation dynamics in these PDMS polymers is well-described by a single-exponential rate law (i.e., $\gamma = 1$). This suggests that the BTBP encounters a relatively homogeneous microdomain and its rotational reorientation is described well by a discrete rotational correlation time.

Figure 3A presents the BTBP rotational reorientation times as a function of PDMS polymer molecular weight. These results show there is an initial increase in the BTBP rotational reorientation time as M_w increases and an apparent leveling off of the probe rotational reorientation time above about $M_w = 10\,000$. In previous work by Stein et al.[19h] on bulk PDMS using the DTES probe, the authors saw somewhat different results. Specifically, the DTES rotational reorientation times were very similar to one another at $M_w = 1250$ and 2000, there was an increase in the rotational reorientation time between $M_w = 2000$ and 3780, and the DTES rotational reorientation dynamics remained indistinguishable above $M_w = 3780$ and up to 28 000. Along with our results (●) in Figure 3, we also show results of the inverse rate of pyrene intermolecular excimer

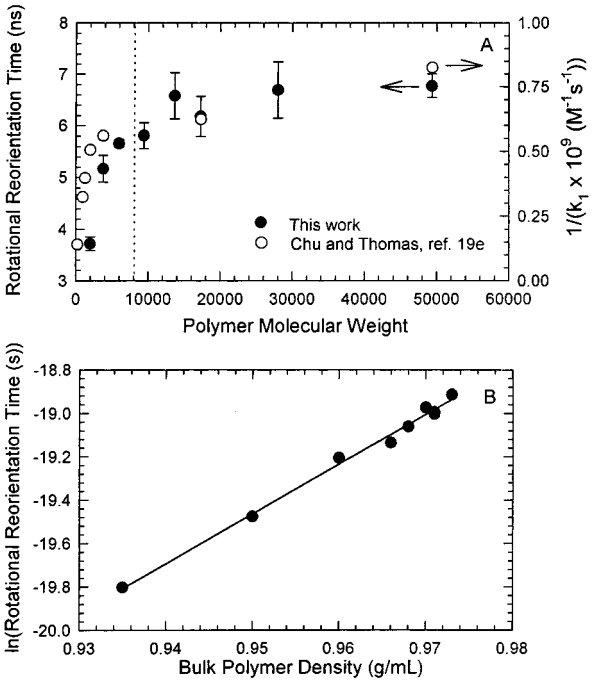

Figure 3. Summary of BTBP dynamics in PDMS. (Panel A) BTBP rotational reorientation times (●) as a function of polymer molecular weight. The dashed line denotes the reported entanglement value (M_e) for PDMS. Results from Chu and Thomas[19e] are also shown (○). (Panel B) Correlation between the BTBP rotational reorientation time and PDMS bulk density. The solid line represents the first-order fit to the data ($r^2 = 0.993$).

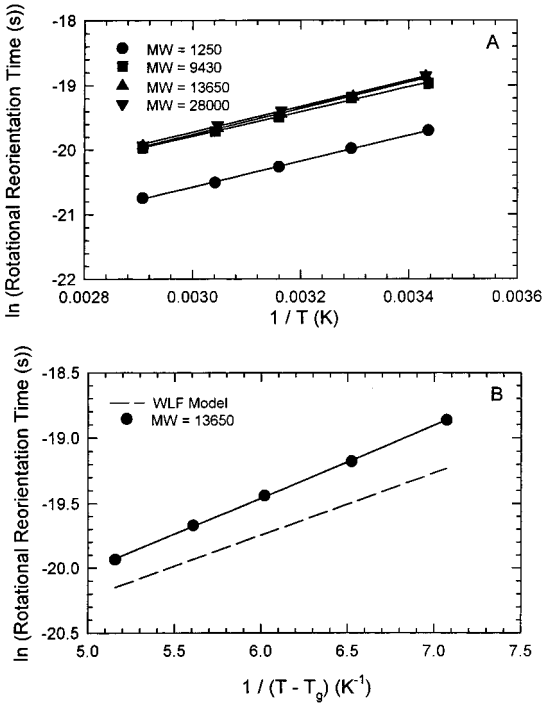

Figure 4. Temperature dependence of the BTBP rotational reorientation dynamics in bulk PDMS. (Panel A) Arrhenius plot for BTBP in bulk PDMS. (Panel B) Williams−Landel−Ferry (WLF) model applied to the $M_w = 13\,650$ PDMS data. The points represent experimental data and the dashed line is the calculated data from the WLF equation.

formation (○) from Chu and Thomas.[19e] The similarity between these data sets and their break points are excellent considering the differences between the measurements and systems.

The entanglement molecular weight (M_e) is characteristic of amorphous polymers and denotes the point where chains become too long to slip past one another easily.[11a,c] An M_e of ~8100 has been reported for PDMS on the basis of the plateau modulus.[11a,29] Other work has reported that local chain dynamics become independent of molecular weight when M_w is greater than 10 000.[30] In this context the results shown in Figure 3A can be explained qualitatively as follows. At low PDMS M_w the dynamics measured by the BTBP probe is a convolution of the segmental chain motions and relaxation from the polymer chain ends. As the chain length and M_w increase, chain entanglement occurs and the BTBP reports from "transient" networks wherein the probe dynamics are controlled by the internal chain dynamics. Above M_e, the internal chain dynamics remain effectively constant and there is no detectable change in the BTBP motion.

To explore the relationship between the BTBP dynamics and the PDMS bulk properties in more detail, we looked for possible correlations between the BTBP dynamics and some physical aspect of the polymer. Chu and Thomas[19e] established a link between the rate constant for pyrene excimer formation and the bimolecular quenching of pyrene by phthalic anhydride or nitrododecanoic acid in PDMS and the PDMS bulk polymer density. Figure 3B presents our BTBP rotational reorientation times as a function of bulk PDMS polymer density. The points are the data from Figure 3A and the solid line is the least squares fit ($r^2 = 0.993$). These results suggest a simple and attractive relationship between the PDMS bulk density and the rotational dynamics of the BTBP probe.

Effect of Temperature on BTBP Rotational Reorientation Dynamics. From temperature-dependent measurements of the BTBP rotational reorientation dynamics, we can determine the activation energy (E_a) associated with the BTBP rotational process in neat PDMS. If E_a is statistically equivalent to the activation energy for polymer viscous flow (E_η) and/or if the rotational reorientation dynamics can be described within the Williams-Landel-Ferry (WLF) framework,[31] then the probe dynamics are coupled to the cooperative segmental chain dynamics (α-relaxations). The WLF expression is given by

$$\ln \phi = \frac{-2.303c_1(T - T_g)}{c_2 + (T - T_g)} + \mathrm{SF} \qquad (15)$$

where c_1 and c_2 are constants for a given polymer (6.1 and 69.0 for PDMS, respectively) and SF is a shift factor to adjust the calculated WLF line to be on the same absolute scale as the experimental data.[31]

Figure 4A presents Arrhenius plots for BTBP dissolved in four molecular weight PDMS polymers. These particular molecular weights were chosen to span the region below, near, and above M_e. Inspection of these results show that, over the temperature range studied, the experimental data is well-represented by an Arrhenius expression. Table 2 collects the individual E_a values for the BTBP rotational reorientation in each of the PDMS polymers studied. Two aspects of these results merit special mention. First, the recovered E_a for BTBP rotational reorientation in the PDMS polymers tested (above and below M_e) are independent of M_w and statistically equivalent to one another (16 kJ/

Table 2. Activation Energies (E_a) for BTBP Rotational Reorientation in PDMS Polymers of Varying Molecular Weight (The Activation Energy for PDMS Viscous Flow (E_η) is 16 ± 1 kJ/mol[19h,21d])

M_w (g/mol)	E_a (kJ/mol)[a]	E_a (kJ/mol)[b]	E_a (kJ/mol)[c]
1250	16.8 ± 0.3	28	
3780		27	
5970			11.9
9430	16.1 ± 0.5		
13 650	16.8 ± 0.4		
28 000	16.6 ± 0.6	27.5	12.4

[a] This work. [b] Reference 19h, using dansyltriethoxysilane (DTES). [c] Reference 19i, using naphthyltriethoxysilane (NTES).

mol) at the 99% confidence interval. Second, the measured E_a from the BTBP rotational reorientation is in excellent agreement with the E_η value for PDMS (16 ± 1 kJ/mol)[19h,21] reported in the literature.

The intercepts for the Arrhenius plots are −5.86 ± 0.10, −4.82 ± 0.18, −5.11 ± 0.14, and −5.02 ± 0.21 for the polymers with M_w of 1250, 9430, 13 650, and 28 000, respectively. These results argue that the frequency factor for the 1250 polymer is statistically different from all other polymers tested and the frequency factor is nearly a decade greater for the 1250 polymer. This suggests that in the lower M_w polymers the absolute reorientational dynamics are governed by E_a, T, and the frequency factor. Above 1250, E_a and T only seem to govern the BTBP rotational reorientation in neat PDMS.

Figure 4B compares the experimental BTBP results on M_w = 13 650 PDMS to the WLF model (- - -). These results clearly demonstrate that the BTBP rotational reorientation data is well-described by the WLF model. We interpret the agreement between the activation processes and the WLF model to indicate that the BTBP reorientation dynamics are coupled well to the cooperative segmental chain dynamics (α-relaxations) in PDMS between M_w = 1250 and 28 000 over the temperature range studied. Further, these results suggest that the friction associated with the longest of the polymer motions is also sensed by the BTBP probe. For comparison, Table 2 includes E_a values determined by Fayer and co-workers[19h,i] using DTES or NTES dissolved in PDMS. From these data it is clear that neither probe studied by Fayer and associates is fully coupled to the cooperative segmental chain dynamics (α-relaxations) in PDMS whereas BTBP is clearly well-coupled to the cooperative chain dynamics.

PDMS in Toulene Solutions. As a prelude to the CO_2 work, we investigated the behavior of BTBP in a series of PDMS/toulene mixtures. The results are summarized in Figure 5. In Figure 5A we show the complete data set from pure bulk PDMS to neat toulene. Figure 5B illustrates the region between a toluene volume fraction (TVF) of zero (bulk PDMS) and 0.12. The results demonstrate that the BTBP rotational reorientational motion increases 3-fold as we go from pure PDMS to PDMS swollen with a TVF of 0.12. On going further from a TVF of 0.12 to neat toulene, we see the reorientational motion increases by about a decade. Thus, in the PDMS/toulene systems, the BTBP dynamics can be adjusted by about a factor of 30, depending on the TVF.

Effect of CO_2 on BTBP Dynamics in PDMS. Figure 6A presents the BTBP rotational reorientation time as a function of CO_2 pressure for several representative molecular weight PDMS polymers at 25.0 °C. Several aspects of this data merit special mention.

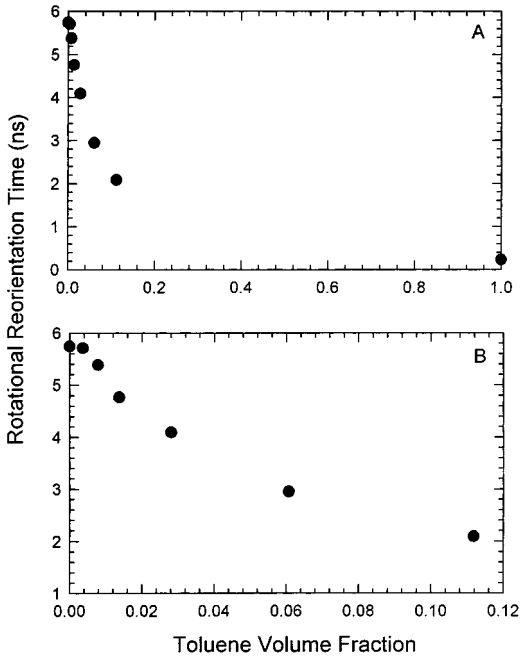

Figure 5. Effects of toulene volume fraction (TVF) on the BTBP rotational reorientation dynamics in PDMS. (Panel A) Full data set at 25.0 °C. (Panel B) Abbreviated data set to TVF of 0.12.

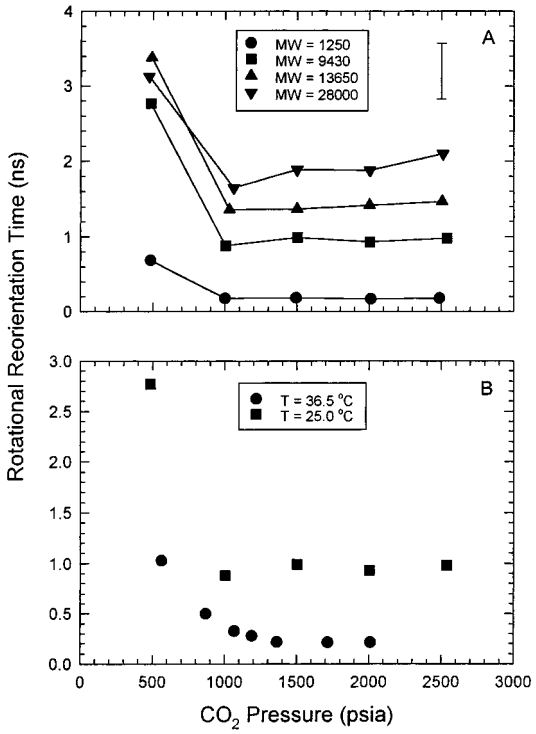

Figure 6. Effects of CO_2 pressure on the BTBP rotational reorientation dynamics in PDMS. (Panel A) BTBP rotational reorientation times as a function of CO_2 pressure at 25.0 °C. The error bar represents the largest measured uncertainty (±2 standard deviation). (Panel B) BTBP rotational reorientation times in PDMS (M_w = 94 30l) as a function of CO_2 pressure at ambient (■, 25.0 °C) and supercritical (●, T = 36.5 °C) conditions.

First, compared to the rotational reorientation times observed in neat PDMS (Figure 3A), the BTBP rotational reorientation time decreases up to 5-fold on the addition of liquid CO_2. It is known that CO_2 can readily swell PDMS[3] and our data is fully consistent with CO_2 dilation and a concomitant decrease in PDMS local

polymer dynamics mediated by the polymer uptake of CO_2 and the molecular motion of the CO_2 itself which serves as diluent and polymer dilator. Second, the BTBP rotational reorientation time decreases on increasing the CO_2 pressure. Third, the BTBP rotational reorientation time drops precipitously between 500 and 1000 psia of CO_2 for all molecular weight polymers and levels off above 1000 psia of CO_2. Examination of the CO_2 phase equilibria at 25.0 °C shows that the gas−liquid phase transition occurs between 500 and 1000 psia.[32] Moreover, it is likely that the solublity limit of the CO_2 in the PDMS is reached at 1000 psia at 25 °C. Thus, we see that the less dense, gaseous CO_2 swells the polymer to a lesser extent than the higher density liquid CO_2.

These results prompted us to question whether the BTBP rotational reorientation dynamics and hence the PDMS polymer could actually be tuned continuously with CO_2 pressure. From the gas/liquid CO_2 experiments, we noted a sharp change in the BTBP rotational reorientation time as we crossed the vapor−liquid equilibrium line. It is well-known that one can adjust continuously CO_2 between gas- and liquid-like densities when it is maintained above its critical temperature (T_c; where T_c = 31.1 °C). Thus, we aimed to determine if we could use the intrinsic tunability of "supercritical CO_2"[33] to adjust continuously the BTBP rotational reorientation dynamics in the PDMS system.

Figure 6B collects the experimental rotational reorientation times for BTBP in PDMS (M_w = 9430) at 25.0 (■) and 36.5 °C (●) as a function of CO_2 pressure. The recovered BTBP rotational reorientation times in the PDMS dilated by supercritical CO_2 are, at the same pressure, statistically lower due to the increase in temperature which subsequently decreases the BTBP rotational reorientation time. More interestingly, closer examination of the T = 36.5 °C data in Figure 6B shows that, instead of the sharp change in rotational reorientation time observed with increasing CO_2 pressure in the ambient system (*vide supra*), we observe a continuous decrease in the BTBP rotational reorientation time with increasing CO_2 pressure. The inherent tunability of the supercritical CO_2 can thus be used to tailor the behavior of the BTBP molecules within the PDMS.

Conclusions

We have shown that BTBP can be used to track cooperative segmental chain dynamics (α-relaxations) within the bulk PDMS system. The BTBP rotational reorientation times scale with polymer molecular weight before leveling off above the known PDMS entanglement value. There is also a simple correlation between BTBP dynamics and the PDMS bulk density. The temperature dependence of the BTBP rotational dynamics in PDMS are Arrhenius activated at all M_w values studied and the activation energies for BTBP rotational reorientation (∼16 kJ/mol) are in excellent agreement with the activation energy for PDMS viscous flow (16 kJ/mol), showing that the local BTBP rotational dynamics correlate well with the macroscopic bulk polymer dynamics. Our results are, however, significantly different compared to the results that Fayer and co-workers found for NTES and DTES in PDMS.[19h,i]

We speculate that the differences between our work and that from the Fayer group arises from two possible factors. First, all the probes used by Fayer and his team are polar and they are likely to exhibit stronger intermolecular interactions with the PDMS polymer subunits relative to BTBP which is nonpolar. Second, the alkoxide residues on Fayer's probes could potentially hydrolyze if they are not maintained in a dry environment.[34] If these probes were to hydrolyze to any extent, the Si−OH formed would provide a sight for possible hydrogen bonding. These types of specific interactions, absent in BTBP, could lead to a stronger temperature dependence for NTES and DTES compared to the activation of PDMS viscous flow alone.

DTES and NTES may also be shorter than the correlation length for the bulk PDMS polymers whereas BTBP is at least equal to if not larger than the PDMS correlation length. The evidence for this is a comparison of the data presented in Figure 6 of ref 19h where differences between the DTES rotational reorientation dynamics are seen between PDMS polymers with M_w = 2000 and 3780 which is well-below the known M_e. In the BTBP system the break point is clearly seen (Figure 3) more near the known M_e and there is a clear correlation between the BTBP rotational reorientation dynamics and the PDMS bulk density. Such a correlation is not seen in the DTES and NTES results. In support of this arguement we have measured the rotational correlation time for perylene (the BTBP parent compound) dissolved in the M_w = 28 000 PDMS sample. Although BTBP and perylene have molar volumes that differ by about a factor of 2−3, we have found that the rotational reorientation time for perylene is 300 (!) times faster compared to BTBP in identical polymer samples under identical conditions.[35]

Addition of CO_2 above its critical temperature allows us to tune continuously the local PDMS polymer dynamics by over a decade. This illustrates that we can clearly tune the dynamics of dopants, reactants, monomers, etc., within polymers by controlling the CO_2 pressure.

Acknowledgment. Financial support for this research was provided by the Division of Chemical Sciences, Office of Basic Energy Sciences, Office of Energy Research, U.S. Department of Energy (DEFGO290-ER14143), the Air Force Office of Scientific Research, Summer Research Extension Program (F49620-93-C-0063), and the ACS Analytical Division Fellowship to E.D.N. sponsored by DuPont Company. We thank C. A. Eckert and B. L. West (Georgia Institute of Technology) for graciously providing us with the polymers used for these experiments.

Supporting Information Available: Tables S-1 through S-11 provide all the experimental BTBP rotational reorientation times, excited-state fluorescence lifetimes, limiting anisotropies, and recovered χ^2 values (7 pages). Ordering information is given on any current masthead page.

References and Notes

(1) (a) McHugh, M. A.; Krukonis, V. J. *Supercritical Fluid Extraction: Principles and Practice,* 2nd ed.; Butterworth-Heinemann: Boston, MA, 1994. (b) Kiran, E. In *Supercritical Fluids. Fundamentals for Application*; Kiran, E., Sengers, J. M. H. L, Eds.; Kluwer Academic: Dordrecht, Germany, 1994.

(2) (a) Yalpani, M. *Polymer* **1993**, *34*, 1102. (b) DeSimone, J. M.; Maury, E. E.; Menceloglu, Y. Z.; McClain, J. B.; Romack, T. J.; Combes, J. R. *Science* **1994**, *265*, 356. (c) Clark, M. R.; DeSimone, J. M. *Macromolecules* **1995**, *28*, 3002. (d) Adamsky, F. A.; Beckman, E. J. *Macromolecules* **1994**, *27*, 312.

(3) (a) Mertsch, R.; Wolf, B. A. *Macromolecules* **1994**, *27*, 3289. (b) Garg, A.; Gulari, E.; Manke, C. W. *Macromolecules* **1994**, *27*, 5643. (c) Xiong, Y.; Kiran, E. *Polymer* **1995**, *36*, 4817. (d)

Bae, Y. C.; Gulari, E. *J. Appl. Polym. Sci.* **1997**, *63*, 459. (e) Gerhardt, L. J.; Manke, C. W.; Gulari, E. *J. Polym. Sci. B: Polym. Phys.* **1997**, *35*, 523.

(4) Paulaitis, M. E.; Krukonis, V. J.; Reid, R. C. *Rev. Chem. Eng.* **1983**, *1*, 179.

(5) (a) Berens, A. R.; Huvard, G. S.; Korsmeyer, R. W.; Kunig, F. W. *J. Appl. Polym. Sci.* **1992**, *46*, 231. (b) Cooper, A. I.; Kazarian, S. G.; Poliakoff, M. *Chem. Phys. Lett.* **1993**, *206*, 175. (c) Poliakoff, M.; Howdle, S. M.; Kazarian, S. G. *Angew Chem., Int. Ed. Engl.* **1995**, *34*, 1275. (d) Shim, J. J.; Johnston, K. P. *AIChE J.* **1989**, *35*, 1097.

(6) Tom, J. W.; Debenedetti, P. G. *Biotechnol. Prog.* **1991**, *7*, 403. (b) Mawson, S.; Johnston, K. P.; Combes, J. R.; DeSimone, J. M. *Macromolecules* **1995**, *28*, 3182. (c) Luna-Barcenas, G.; Kanakia, S. K.; Sanchez, I. C.; Johnston, K. P. *Polymer* **1995**, *36*, 3173.

(7) Watkins, J. J.; McCarthy, T. J. *Macromolecules* **1994**, *27*, 4845. (b) Watkins, J. J.; McCarthy, T. J. *Macromolecules* **1995**, *28*, 4067.

(8) (a) Via, J.; Taylor, L. T. *CHEMTECH* **1993**, *24* (11), 38. (b) A presidential directive published in the *Federal Register* (S8 FR: 65018; Dec. 10, 1993), implemented Jan. 1, 1996.

(9) (a) *Supercritical Fluid Science and Technology;* Johnston, K. P.; Penninger, J. M. L., Eds.; ACS Symposium Series 406; American Chemical Society: Washington, DC, 1989. (b) *Supercritical Fluid Technology—Reviews in Modern Theory and Applications;* Bruno, T. J., Ely, J. F., Eds.; CRC Press: Boca Raton, FL, 1991. (c) *Supercritical Fluid Technology—Theoretical and Applied Approaches in Analytical Chemistry;* Bright, F. V., McNally, M. E. P., Eds.; ACS Symposium Series 488; American Chemical Society: Washington, DC, 1992. (d) *Supercritical Fluid Engineering Science—Fundamentals and Applications*; Kiran, E., Brennecke, J. F., Eds.; ACS Symposium Series 514; American Chemical Society: Washington, DC, 1993.

(10) (a)Vieth, W. R. *Diffusion In and Through Polymers. Principles and Applications*; Hans Werlar: Munich, 1991. (b) Van Krevelen, D. W. *Properties of Polymers*; Elsevier: New York, 1990. (c) Durrill, P. L.; Griskey, R. G. *AIChE J.* **1966**, *12*, 1147. (d) Wang, W.-C.; Kramer, E. J.; Sachse, W. H. *J. Polym. Sci.* **1982**, *20*, 1371. (e) Koros, W. J. *Polym. Sci., Polym. Phys. Ed.* **1985**, *23*, 1611. (f) Berens, A. R.; Huvard, G. S. In *Supercritical Fluid Science and Technology*; Johnston, K. P., Penninger, J. M. L., Eds.; ACS Symposium Series 406; American Chemical Society: Washington, DC, 1989. (g) Fleming, G. K.; Koros, W. J. *Macromolecules* **1986**, *19*, 2285. (h) Chiou, J. S.; Paul, D. R. *J. Membr. Sci.* **1989**, *45*, 167. (i) Condo, P. D.; Sanchez, I. C.; Panayiotou, C. G.; Johnston, K. P. *Macromolecules* **1992**, *25*, 6119. (j) Pope, D. S.; Koros, W. J.; Hopfenberg, H. B. *Macromolecules* **1994**, *27*, 5839. (k) Handa, Y. P.; Lampron, S.; O'Neill, M. L. *J. Polym. Sci. B: Polym. Phys.* **1994**, *32*, 2549. (l) Wessling, M.; Mulder, M. H. V.; Bos, A.; van der Linden, M.; Bos, M.; van der Linden, W. E. *J. Membr. Sci.* **1994**, *86*, 193. (m) Ghosal, K.; Chern, R. T.; Freeman, B. D.; Daly, W. H.; Negulescu, I. I. *Macromolecules* **1996**, *29*, 4360. (n) Shieh, Y.-T.; Su, J.-H.; Manivannan, G.; Lee, P. H. C.; Sawan, S. P.; Spall, W. D. *J. Appl. Polym. Sci.* **1996**, *59*, 695. (o) Kazarian, S. G.; Vincent, M. F.; Bright, F. V.; Liotta, C. L.; Eckert, C. A. *J. Am. Chem. Soc.* **1996**, *118*, 1729.

(11) (a) Flory, P. J. *Principles of Polymer Chemistry*; Cornell University Press: Ithaca, NY, 1969. (b) *Silicon Based Polymer Science*; Zeigler, J. M., Fearon, F. W. G., Eds.; Advances in Chemistry Series 224; American Chemical Society: Washington, DC, 1990. (c) Sperling, L. H. *Introduction to Physical Polymer Science*, 2nd ed.; Wiley Interscience: New York, 1992.

(12) (a) Davies, M.; Edwards, A. *Trans. Faraday Soc.* **1967**, *63*, 2163. (b) Hains, P. J.; Williams, G. *Polymer* **1975**, *16*, 725. (c) Dhinojwala, A.; Wong, G. K.; Torkelson, J. M. *Macromolecules* **1993**, *26*, 5943. (d) Mansour, A. A.; Stoll, B. *Colloid. Polym. Sci.* **1992**, *270*, 219. (e) Dhinojwala, A.; Wong, G. K.; Torkelson, J. M. *J. Chem. Phys.* **1994**, *100*, 6046. (f) Kirst, K. U.; Kremer, F.; Pakula, T.; Hollingshurst, J. *Colloid Polym. Sci.* **1994**, *272*, 1420. (g) Roland, C. M.; Nagi, K. L. *Macromolecules* **1996**, *29*, 5747.

(13) (a) McLoughlin, K.; Szeto, C.; Duncan, T. M.; Cohen, C. *Macromolecules* **1996**, *29*, 5475. (b) Cosgrove, T.; Turner, M. J.; Griffiths, P. C.; Hollingshurst, J.; Shenton, M. J.; Semlyen, J. A. *Polymer* **1996**, *37*, 1535. (c) Zhu, W.; Ediger, M. D. *Macromolecules* **1997**, *30*, 1205.

(14) Shimada, S. *Prog. Polym. Sci.* **1992**, *17*, 1045.

(15) (a) Lamarre, L.; Sung, C. S. P. *Macromolecules* **1983**, *16*, 1729. (b) Victor, J. G.; Torkelson, J. M. *Macromolecules* **1987**, *20*, 2241. (c) Victor, J. G.; Torkelson, J. M. *Macromolecules* **1987**, *20*, 2951. (d) Victor, J. G.; Torkelson, J. M. *Macromolecules* **1988**, *21*, 3490. (e) Yu, W. C.; Sung, C. S. P.; Robertson, R. E. *Macromolecules* **1988**, *21*, 355. (f) Royal, J. S.; Victor, J. G.; Torkelson, J. M. *Macromolecules* **1992**, *25*, 4792. (g) Royal, J. S.; Torkelson, J. M. *Macromolecules* **1992**, *25*, 4792. (h) Kanato, H.; Tran-Cong, Q.; Hua, D. H. *Macromolecules* **1994**, *27*, 7907. (i) Tran-Cong, Q.; Chikaki, S.; Kanato, H. *Polymer* **1994**, *35*, 4465.

(16) (a) Dhinojwala, A.; Wong, G. W.; Torkelson, J. M. *Macromolecules* **1992**, *25*, 7395. (b)Hooker, J. C.; Torkelson, J. M. *Macromolecules* **1995**, *28*, 7682. (c) Hall, D. B.; Hooker, J. C.; Torkelson, J. M. *Macromolecules* **1997**, *30*, 667.

(17) (a) Blackburn, F. R.; Cicerone, M. T.; Hietpas, G.; Wagner, P. A.; Ediger, M. D. *J. Non-Cryst. Solids* **1994**, *172−174*, 256. (b) Blackburn, F. R.; Cicerone, M. T.; Ediger, M. D. *J. Polym. Sci. B: Polym. Phys.* **1994**, *32*, 2595. (c) Inoue, T.; Cicerone, M. T.; Ediger, M. D. *Macromolecules* **1995**, *28*, 3425. (d) Ediger, M. D.; Inoue, T.; Cicerone, M. T.; Blackburn, F. R. *Macromol. Symp.* **1996**, *101*, 139.

(18) (a) Jarry, J. P.; Monnerie, L. *Macromolecules* **1979**, *12*, 927. (b) Liao, T.-P.; Morawetz, H. *Macromolecules* **1980**, *13*, 1228. (c) Pajot-Augy, E.; Bokobza, L.; Monnerie, L.; Castellan, A.; Bouas-Laurent, H. *Macromolecules* **1984**, *17*, 1490. (d) Jarry, J. P.; Erman, B.; Monnerie, L. *Macromolecules* **1986**, *19*, 2750. (e) Itagaki, H. *Macromolecules* **1991**, *24*, 6531. (f) Royal, J. S.; Torkelson, J. M. *Macromolecules* **1993**, *26*, 5331. (g) Leezenberg, P. B.; Frank, C. W. *Chem. Mater.* **1995**, *7*, 1784. (h) Leezenberg, P. B.; Frank, C. W. *Macromolecules* **1995**, *28*, 7407. (i) Itoh, T.; Yang, M.-H.; Chou, C. *J. Chem. Soc., Faraday Trans.* **1996**, *92*, 3593.

(19) (a) Viovy, J. L.; Monnerie, L.; Merola, F. *Macromolecules* **1985**, *18*, 1130. (b)Viovy, J. L.; Frank, C. W.; Monnerie, L. *Macromolecules* **1985**, *18*, 2606. (c) Ediger, M. D.; Domingue, R. P.; Peterson, K. A.; Fayer, M. D. *Macromolecules* **1985**, *18*, 1182. (d) Hyde, P. D.; Ediger, M. D.; Kitano, T.; Ito, K. *Macromolecules* **1989**, *22*, 2253. (e) Chu, D. Y.; Thomas, J. K. *Macromolecules* **1990**, *23*, 2217. (f) Ediger, M. D. *Annu. Rev. Phys. Chem.* **1991**, *42*, 225. (g) Stein, A. D.; Hoffman, D. A.; Frank, C. W.; Fayer, M. D. *J. Chem. Phys.* **1992**, *96*, 3269. (h) Stein, A. D.; Hoffmann, D. A.; Marcus, A. H.; Leezenberg, P. B.; Frank, C. W.; Fayer, M. D. *J. Phys. Chem.* **1992**, *96*, 5255. (i) Diachun, N. A.; Marcus, A. H.; Hussey, D. M.; Fayer, M. D. *J. Am. Chem. Soc.* **1994**, *116*, 1027. (j) Ono, K.; Okada, Y.; Yokotsuka, S.; Ito, S.; Yamamoto, M. *Polym. J.* **1994**, *26*, 199. (k) Soutar, I.; Swanson, L. *Macromol. Symp.* **1995**, *90*, 267. (l) Hoffman, D. A.; Anderson, J. E.; Frank, C. W. *J. Mater. Chem.* **1995**, *5*, 13. (m) Ono, K.; Ueda, K.; Sasaki, T.; Murase, S.; Yamamoto, M. *Macromolecules* **1996**, *29*, 1584. (n) Soutar, I.; Swanson, L.; Christensen, R. L.; Drake, R. C.; Phillips, D. *Macromolecules* **1996**, *29*, 4931. (o) Leezenberg, P. B.; Fayer, M. D.; Frank, C. W. *Pure Appl. Chem.* **1996**, *68*, 1381. (p) Leezenberg, P. B.; Marcus, A. H.; Frank, C. W.; Fayer, M. D. *J. Phys. Chem.* **1996**, *100*, 7646. (q) Soutar, I.; Jones, C.; Lucas, D. M.; Swanson, L. *J. Photochem. Photobiol., A—Chem.* **1996**, *102*, 87.

(20) (a) Winnik, M. A. In *Photophysical and Photochemical Tools in Polymer Science*; Winnik, M. A., Ed.; Reidel: Dordrecht, The Netherlands, 1986; pp 467−494. (b) Char, K.; Gast, A. P.; Frank, C. W. *Langmuir* **1988**, *4*, 989. (c) Németh, S.; Jao, T.-C.; Fendler, J. H. *Macromolecules* **1994**, *27*, 5449. (d) Asano, M.; Winnik, F. M.; Yamashita, T.; Horie, K. *Macromolecules* **1995**, *28*, 5861.

(21) Allen, G. *J. Appl. Chem.* **1964**, *14*, 1.

(22) (a) Gratton, E.; Jameson, D. M.; Hall, R. D. *Annu. Rev. Biophys. Bioeng.* **1984**, *13*, 105. (b) Jameson, D. M.; Gratton, E.; Hall, R. D. *Appl. Spectrosc. Rev.* **1984**, *20*, 55. (c)Bright, F. V.; Betts, T. B.; Litwiler, K. S. *CRC Crit. Rev. Anal. Chem.* **1990**, *21*, 389. (d) Bright, F. V. *Appl. Spectrosc.* **1995**, *49*, 14A.

(23) (a) Ben-Amotz, D.; Drake, J. M. *J. Chem. Phys.* **1988**, *89*, 2. (b) Williams, A. M.; Ben-Amotz, *D. Anal. Chem.* **1992**, *64*, 700. (c) Heitz, M. P.; Bright, F. V. *J. Phys. Chem.* **1996**, *100*, 6889.

(24) (a) Mantulin, W. W.; Weber, G. *J. Chem. Phys.* **1977**, *66*, 4092. (b) Barkley, M. D.; Kowalczyk, A. A.; Brand, L. *J. Biol. Chem.* **1981**, *75*, 3581. (c) Lakowicz, J. R.; Cherek, H.; Maliwal, B. P.; Gratton, E. *Biochemistry* **1985**, *24*, 376.

(25) Betts, T. A.; Bright, F. V. *Appl. Spectrosc.* **1990**, *44*, 1190.

(26) Spencer, R. D.; Weber, G. *J. Chem. Phys.* **1970**, *52*, 1654.

(27) Heitz, M. P.; Bright, F. V. *Appl. Spectrosc.* **1995**, *49*, 20.

(28) Beecham, J. M.; Gratton, E.; Ameloot, M.; Knutson, J. R.; Brand, L. In *Topics in Fluorescence Spectroscopy*; Lakowicz, J. R., Ed.; Plenum Press: New York, 1991; Vol. 2.
(29) Stepto, R. F. T. *Eur. Polym. J.* **1993**, *29*, 415.
(30) Heatley, F. *Prog. Nucl. Magn. Reson. Spectrosc.* **1979**, *13*, 47.
(31) Ferry, J. D. *Viscoelastic Properties of Polymers*, 3rd ed.; John Wiley and Sons: New York, 1980.
(32) Reid, R. C.; Prausnitz, J. M.; Poling, B. E. *The Properties of Gases and Liquids*, 4th ed.; McGraw-Hill: New York, 1986.
(33) Although the CO_2 is above its critical temperature, the system is not supercritical.
(34) (a) Hench, L. L.; West, J. K. *Chem. Rev.* **1990**, *90*, 33−72. (b) Brinker, C. J.; Scherer, G. W. *Sol-Gel Science*; Academic Press: New York, 1989.
(35) Perylene is the classical anisotropic rotor.[24] It is possible that the PDMS precludes the slower of perylene's rotational motions (out of plane) and only the faster (in plane) motion is observed. There is no evidence for this scenario, but experiments to address such are in progress.

MA970335+